PHF1 Tudor and N-terminal domains synergistically target partially unwrapped nucleosomes to increase DNA accessibility

Matthew D. Gibson[1], Jovylyn Gatchalian[2], Andrew Slater[1], Tatiana G. Kutateladze[2] and Michael G. Poirier[1,3,4,*]

[1]Department of Physics, Ohio State University, Columbus, OH 43210, USA, [2]Department of Pharmacology, University of Colorado School of Medicine, Aurora, CO 80045, USA, [3]Biophysics Graduate Program, Ohio State University, Columbus, OH 43210, USA and [4]Department of Chemistry and Biochemistry, Ohio State University, Columbus, OH 43210, USA

ABSTRACT

The Tudor domain of human PHF1 recognizes trimethylated lysine 36 on histone H3 (H3K36me3). PHF1 relies on this interaction to regulate PRC2 methyltransferase activity, localize to DNA double strand breaks and mediate nucleosome accessibility. Here, we investigate the impact of the PHF1 N-terminal domain (NTD) on the Tudor domain interaction with the nucleosome. We show that the NTD is partially ordered when it is natively attached to the Tudor domain. Through a combination of FRET and single molecule studies, we find that the increase of DNA accessibility within the H3K36me3-containing nucleosome, instigated by the Tudor binding to H3K36me3, is dramatically enhanced by the NTD. We demonstrate that this nearly order of magnitude increase is due to preferential binding of PHF1 to partially unwrapped nucleosomes, and that PHF1 alters DNA–protein binding within the nucleosome by decreasing dissociation rates. These results highlight the potency of a PTM-binding protein to regulate DNA accessibility and underscores the role of the novel mechanism by which nucleosomes control DNA–protein binding through increasing protein dissociation rates.

INTRODUCTION

The organization of eukaryotic DNA into nucleosomes sterically occludes DNA-binding complexes that regulate DNA processing including transcription (1), replication (2) and repair (3). Posttranslational modification (PTM) of the histone proteins that wrap DNA into nucleosomes regulate numerous aspects of nucleosome function (3). There are over 500 different histone PTMs (4,5) located throughout the nucleosome, which can function individually or in combination (6). Histone PTMs function by two general mechanisms: (i) the histone code mechanism (7,8) where a histone PTM provides a specific binding site for recruiting chromatin modifying complexes including chromatin remodelers and histone modifying enzymes, and (ii) the nucleosome dynamics mechanism (9,10) where a histone PTM directly alters chromatin properties including chromatin compaction, nucleosome unwrapping and nucleosome stability. Recently, we reported that these mechanisms can function in combination where the binding of the Tudor domain of the human Plant Homeodomain (PHD) finger protein 1 (PHF1) to H3K36me3 increases nucleosomal DNA accessibility (11).

PHF1 is a 456 amino acid (aa) protein (Figure 1A) that is involved in transcriptional regulation (12,13) and DNA repair (14). It contains an N-terminal domain (aa 2–28) of unknown function, a Tudor domain (aa 28–87) that specifically recognizes H3K36me3 (15–18), and two PHD domains (aa 87–140 and aa 189–240) that may facilitate interaction with EZH2 (19), the methyltransferase subunit of the Polycomb repressive complex, PRC2 (20,21). Interaction with H3K36me3 stabilizes PHF1 at DNA double strand breaks together with the DNA repair complexes PARP1 and Ku70-Ku80 (15). Separately, binding of PHF1 Tudor to H3K36me3 results in a reduction of H3K27 trimethylation by the gene silencing complex PRC2 (15,22–23). Our finding that binding of PHF1 Tudor to H3K36me3 increases DNA accessibility (11) suggested that PHF1 may function to facilitate transcription or prevent spreading of repressive chromatin by more than one mechanism. However, the mechanistic basis by which PHF1 Tudor increases accessibility and how additional PHF1 domains influence this function remains unknown.

*To whom correspondence should be addressed. Tel: +1 614 247 4493; Fax: +1 614 292 7557; Email: mpoirier@mps.ohio-state.edu
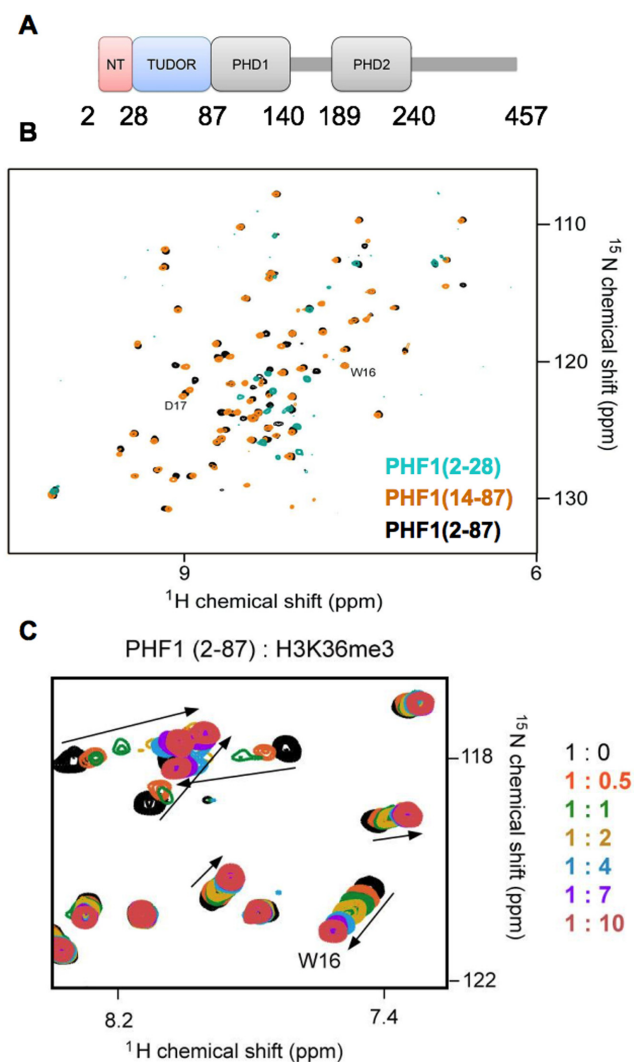
Figure 1. The PHF1 NTD is partially structured and does not affect binding of the adjacent Tudor domain to H3K36me3. (**A**) Diagram showing the known domains in PHF1. (**B**) ^{1}H, ^{15}N HSQC spectral overlays for PHF1(2-28) (teal), PHF1(14–87) (orange), and PHF1(2–87) (black). (**C**) ^{1}H, ^{15}N HSQC spectral overlays of wild type PHF1 NTD-Tudor upon titration with H3K36me3 peptide. The spectra are color-coded according to the protein:peptide molar ratio.

Here, we report on the cooperativity between the NTD and the adjacent Tudor domain of PHF1 in the regulation of nucleosome accessibility. We use NMR and circular dichroism (CD) to find that the NTD is partially structured when linked to the neighboring Tudor and that the NTD does not enhance Tudor binding to H3K36me3. We use ensemble Förster Resonance Energy Transfer (FRET) measurements to determine that the combination of NTD with the Tudor domain, PHF1(2–87) (or NTD-Tudor), dramatically increases nucleosome accessibility by nearly an order of magnitude. We demonstrate this increase is due to an ∼8-fold preference of PHF1 NTD-Tudor to bind partially unwrapped nucleosomes. Using single molecule FRET (sm-FRET) measurements, we find that the increase of DNA accessibility is due to a reduction of DNA-binding protein dissociation rate instead of an increase in DNA unwrap-

ping that would increase the DNA–protein binding rate. This finding highlights our recently reported novel mechanism for the regulation of nucleosome accessibility by altering DNA-binding protein dissociation. Importantly, these studies reveal that PTM binding domains can function not only to recruit their host proteins and protein complexes to chromatin, but can also directly regulate nucleosome dynamics.

MATERIALS AND METHODS

PHF1 constructs and purification

PHF1(14–87) and PHF1(28–87) were cloned as previously described (15). PHF1(2–28) and PHF1(2–87) were generated by amplification of construct of interest from PHF1 cDNA (Open Biosystems) with BamHI and XhoI restriction sites and ligation into pGex6P1 expression vector. Proteins were expressed and purified, essentially as described (15).

Nuclear magnetic resonance

NMR experiments were recorded at 298 K on a Varian INOVA 600 MHz spectrometer equipped with a cryogenic probe. Chemical shift perturbation experiments were carried out using 0.1 mM uniformly ^{15}N-labeled protein in 50 mM Tris pH 6.9, 150 mM NaCl, 2 mM DTT with 5% D$_2$O. The ^{1}H,^{15}N heteronuclear single quantum coherence (HSQC) spectra were recorded in the presence of increasing concentrations of histone H3K36me3 (24–32) peptide synthesized by the University of Colorado Denver Biophysics Core Facility.

Circular dichroism

CD spectra were obtained using a Jasco J-815 spectropolarimeter. PHF1(2–87), PHF1(14–87) and PHF1(28–87) CD spectra were acquired at room temperature in 0.25 nm steps with an illumination bandwidth of 1 nm and a scanning speed of 200 nm/min. Samples were measured in 5 mM potassium phosphate pH 7.5, which was filtered and degassed to reduce buffer absorbance. CD spectra were then analyzed using the software package CDPro (33).

MLA deposition on histones

Histone H3.2(C110A, K36C) was generated by site-directed mutagenesis using a Stratagene QuickChange lightning kit. The histone was then expressed in *Escherichia coli* and purified as previously described (34). The MLA was attached to the sole cysteine present in the mutant H3.2(C110A,K36C) following previously reported protocols (35). Briefly, 5 mg of histones are unfolded in 980 μl of alkylation buffer (1 mM HEPES pH 7.8, 4 M guanidine–HCl, 10 mM D/L-methionine) for 1 h. After unfolding, histones were reduced in 6.66 mM dithiolthreitol (DTT) for 1 h at 37°C. One hundred milligram of (2-bromoethyl) trimethylammonium bromide was added to the histones and the reaction was covered and stirred for 5 h at 50°C. The reaction was quenched with 50 μl of 14.3 μM 2-mercaptoethanol (BME). Histones

were then dialyzed against 3 mM BME, lyophylized, re-suspended in water, and dried via vacuum concentration. Labeling efficiency was confirmed by MALDI-TOF mass spectrometry.

Preparation of FRET-labeled histone octamer

Human histones H2A(K119C), H2B, H3.2(C110A), H3.2(C110A,K36C) and H4 were expressed and purified as previously reported (34). Histone heterodimer, H2A(K119C) and H2B, were then refolded separately from tetramer, H3.2(C110A) and H4 or H3.2K$_C$36me3(C110A) and H4, by dialysis from unfolding buffer (7 M guanidine–HCl, 10 mM Tris–HCl pH 7.5, 10 mM DTT) to refolding buffer (5 mM PIPES pH 6.1, 2 M NaCl).

Heterodimer was then labeled with Cy5-maleimide (GE Healthcare) and purified as previously reported (11,36–38). Heterodimer and tetramer were then combined to a molar ratio of 1:2.2 tetramer:heterodimer. The proteins were allowed to complex overnight at 4°C while gently rotating. The resulting octamer was then purified by size exclusion chromatography with a superdex 200 column. Histone octamer was concentrated in a 30 kDa MWCO Amicon Ultra (Millipore) and stored on ice.

Preparation of labeled DNA

Nucleosomal DNA was prepared by PCR from a plasmid containing the 601 sequence with a LexA binding site located at bases 8–27. PCR primers for ensemble experiments were the cy3-labeled oligonucleotide, Cy3-CTGGAGATACTGTATGAGCATACAGTACAATT GGTC and the unlabeled reverse primer ACAGGATG TATATATCTGACACGTGCCTGGAGACTA. Single molecule experiments used the biotinylated reverse primer Biotin-CGCATGCTGCAGACGCGTTACGTATCG which extends the 147 bp 601 sequence with a 75 bp linker and provides the biotin attachment point for use in single molecule experiments. Cy3-labeled oligos were labeled with Cy3 NHS ester (GE Healthcare) at an amino group attached to the 5′ end of the DNA oligo. Primers were then HPLC purified on a 218TP C18 column (Grace/Vydac). After PCR, dsDNA molecules were purified by HPLC on a MonoQ (GE Healthcare) ion exchange column.

Preparation of nucleosomes

Cy3-labeled DNA and Cy5-labeled histone octamer were combined and reconstituted by double salt dialysis and purified on a 5–30% sucrose gradient as previously described (37). Fractions containing nucleosomes were then collected and concentrated with a 30 kDa MWCO Amicon Ultra (Millipore). Supplementary Figure S1 displays reconstituted nucleosomes before and after purification by sucrose gradient.

Preparation of LexA

LexA was expressed and purified by known methods (39). Briefly, LexA was expressed in *E. coli*. LexA was then separated from genomic DNA and the proteome by polyetheleneimine (Sigma) precipitation followed by salting out

LexA with ammonium sulfate. LexA was resuspended in buffer B (20 mM potassium phosphate pH 7, 0.1 mM EDTA, 10% glycerol, 1 mM DTT) + 200 mM NaCl and purified by a linear gradient to B + 800 mM NaCl over either a cellulose phosphate or HiTrap Heparin HP Column (Ge Healthcare, cellulose phosphate discontinued). Final LexA purification was performed on a hydroxyapatite column and dialyzed into storage buffer (10 mM PIPES pH 7.0, 0.1 mM EDTA, 10% v/v glycerol, 200 mM NaCl).

Ensemble FRET measurements

Ensemble FRET efficiencies were determined from spectra acquired by a Horiba Scientific Fluoromax 4. Samples were excited at 510 and 610 nm and the fluorescence spectra were measured from 530 to 750 and 630 to 750 nm for donor and acceptor excitations, respectively. Each wavelength was integrated for 1 s, and the excitation and emission slit width were set to 5 nm with 2 nm emission wavelength steps. FRET measurements were computed though the (ratio)$_A$ method (39,24). Titrations were carried out in 75 mM NaCl, 0.1 mM potassium phosphate pH 7.5, 11.5 mM Tris–HCl pH 7.5, 0.00625% (v/v) Tween20. LexA titrations were fit to $E = (E_f - E_0)/(1 + S_{l_2}/C) + E_0$ where E is the FRET efficiency at concentration C of LexA, E_f is the FRET efficiency at high concentration of titrant and E_0 is the efficiency in the absence of the titrant and S_{l_2} is the inflection point. Errors represent a standard deviation based on three experiments. Fit errors represent 68% confidence bounds. Figure 2D is fit to the equation $S_{l_2}^{PHF1} = \frac{K_D^{PL/P}(K_D^P+[P])}{2K_D^P K_D^{PL/P}+(K_D^L+K_D^{PL/P})[P]}$, and Figure 3H is fit to the equation $S_{l_2}^{LexA} = \frac{K_D^L K_D^{PL/P}(K_D^P+[P])}{K_D^P K_D^{PL/P}+K_D^L[P]}$, where $S_{l_2}^{LexA}$ and $S_{l_2}^{PHF1}$ are the inflection points of LexA and PHF1, respectively as predicted by the four state model presented. K_D^P, K_D^L, $K_D^{PL/P}$ are the dissociation constants of PHF1 2–87 to nucleosomes, LexA to nucleosomes, and LexA to a PHF1 2–87–nucleosome complex, respectively.

Electromobility shift assay

DNA containing the LexA recognition site was incubated at 1 nM with 0–1000 nM LexA and no PHF1, 100 μM PHF1(2–87), 100 μM PHF1(14–87) or 100 μM PHF1(28–87) in 0.5× TE for 10 min at room temperature and resolved by electrophoretic mobility shift assay (EMSA) with a native 5% polyacrylamide gel in 0.3× TBE.

Single molecule FRET measurements

Single molecule measurements were performed as previously described (38,25–26). Briefly, biotinylated sample nucleosomes were allowed to incubate in flow cells at room temperature for 5 min and washed out with imaging buffer containing the desired concentration of LexA and PHF1 truncation. Imaging buffer was 50 mM Tris pH 8.0, 75 mM NaCl, 10% (v/v) glycerol, 0.005% (v/v) Tween20, 0.1 mg/ml BSA, 2 mM Trolox, 0.0115% (v/v) cyclooctatetraene, 0.012% (v/v) 3-nitrobenzyl alcohol, 1.6% (w/v) glucose, 450 μg/ml glucose oxidase, 22 μg/ml catalase.
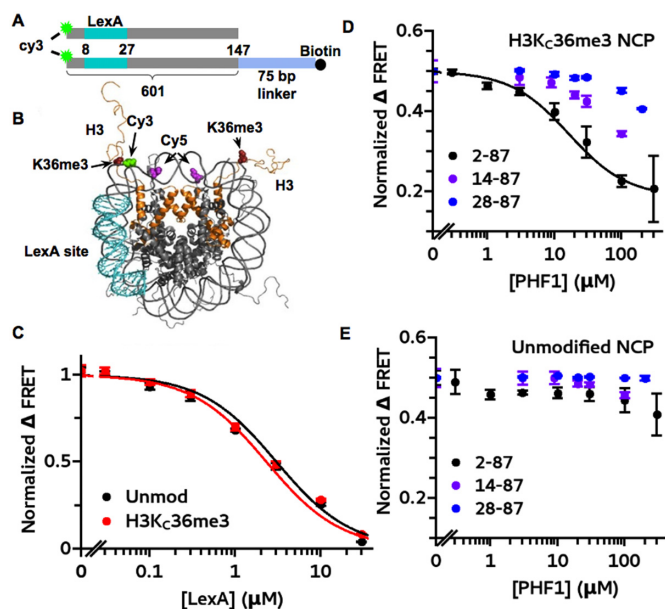
Figure 2. The PHF1 NTD enhances the impact of the Tudor domain on nucleosome accessibility. (**A**) Diagram of DNA molecules used to reconstitute nucleosomes. DNA used for ensemble (top) and single molecule (bottom) measurements. (**B**) Crystal structure of the NCP (PDB ID: 1KX5) that indicates the positions of H3 (orange); MLA at H3K36C (dark red); Cy5 at H2AK119C (purple); LexA binding site (teal). (**C**) FRET efficiencies of LexA titrations with H3K$_C$36me3 (red) and unmodified (black) nucleosomes. Titrations were performed in triplicate and fit to a noncooperative binding isotherm. (**D, E**) FRET efficiencies of PHF1(2–87) (black), PHF1(14–87) (purple), and PHF1(28–87) (blue) titrations with constant [LexA] = $S_{i_{1/2}}$ to H3K$_C$36me3 (**D**) or unmodified (**E**) nucleosomes. Error bars represent a standard deviation based on three experiments.

Time series were selected and generated by custom software and fit to a two-state step function by the vbFRET (27) Matlab program. Idealized time series were further analyzed by custom software to determine dwell-time distributions and the fraction of time nucleosomes spend bound by LexA. Dwell time distributions yield kinetic measurements while the fraction of time bound provides an important control to single molecule experiments because it is analogous to the normalized change in FRET observed in ensemble experiments. The nucleosome is closely tethered to a quartz surface which can alter its behavior. In order to ensure the tethering does not have a significant impact on kinetic measurements it is necessary to compare the ensemble and single molecule behavior of our system. This comparison is shown in Supplementary Figure S2.

RESULTS

The PHF1 NTD is partially structured when linked to Tudor

PHF1 contains a 28-residue tail N-terminal to the Tudor domain, for which the structure and biological role have not been investigated. To examine the PHF1 NTD conformation, we generated an isolated NTD construct, produced uniformly ^{15}N-labeled protein, and recorded its ^{1}H,^{15}N HSQC spectrum. A low dispersion of amide resonances in the spectrum, particularly in the ^{1}H dimension, indicated that the isolated N-terminal tail of PHF1 is largely disor-

dered (Figure 1B, cyan). However, when NTD was physically linked to the Tudor domain in the construct containing residues 2–87 of PHF1, a significant dispersion of all amide resonances was observed, indicating that the NTD-Tudor region (black spectrum) becomes structured. A substantial overlap of resonances in ^{1}H,^{15}N HSQC spectra of PHF1(2–87) and PHF1(14–87) suggested that Tudor can promote folding even in the partially truncated NTD (compare orange and black spectra). The more rigid conformation of NTD when attached to Tudor was supported by analysis of the secondary structure elements in CD spectra of PHF1. We recorded and compared CD spectra of PHF1(2–87), PHF1(14–87) and the PHF1(28–87) domain. As shown in Supplementary Figure S3, the beta strand content in PHF1(2–87) is increased compared with the beta strand content in the PHF1(28–87) domain only or in PHF1(14–87), which also shows increased beta strand content relative to PHF1(28–87).

To determine the effect of NTD on the interaction of the Tudor domain with H3K36me3, we carried out NMR titration experiments. Gradual addition of the H3K36me3 peptide (residues 31–40 of H3) to PHF1(2–87) resulted in large changes in chemical shifts of the protein (Figure 1C). As expected, resonances of the Tudor residues were perturbed utmost, particularly those involved in the formation of the H3K36me3-binding pocket, such as Y47 and E66. However, resonances of several NTD residues, including W16 and D17, which were previously assigned in PHF1(14–87) (15), were also perturbed. The pattern of chemical shift changes was essentially identical to that of seen upon titration of H3K36me3 peptide into the PHF1(14–87) sample, indicating that the binding affinity of Tudor for H3K36me3 is not affected by the presence of the entire NTD (Supplementary Figure S4A). Because the N-terminal region of Tudor along with the adjacent NTD are positioned on the side opposite to the H3K36me3-binding site of Tudor (Supplementary Figure S4B), the observed perturbations likely point to a conformational change that may accompany the interaction rather than a direct involvement of the NTD in binding of the Tudor domain to H3K36me3.

PHF1 NTD-Tudor does not shift nucleosomes into a largely unwrapped state

PHF1-Tudor makes direct contacts with H3 residues 32–40 (15). Since H3 residues 36–40 are located between the 2 DNA gyres in the DNA entry-exit region of the nucleosome, the nucleosome may need to partially unwrap for PHF1-Tudor to bind the H3K36me3 tail. Using FRET (24), we previously found that the Tudor domain alone, PHF1(28–87), does not induce detectable changes to nucleosome unwrapping (11). Still, we considered the possibility that the PHF1-NTD could influence the effect of PHF1-Tudor on nucleosome unwrapping.

We prepared nucleosomes that contain the Widom 601 nucleosome positioning sequence (28) and a Cy3 label at one of the 5 prime ends (Figure 2A). The nucleosome is also labeled with a Cy5 fluorophore at H2A(K119C) (Figure 2B), so fully wrapped nucleosomes undergo efficient Cy3-Cy5 FRET. We prepared and purified Cy3-Cy5 labeled nucleosomes with and without a trimethyl-lysine mimic at ly-
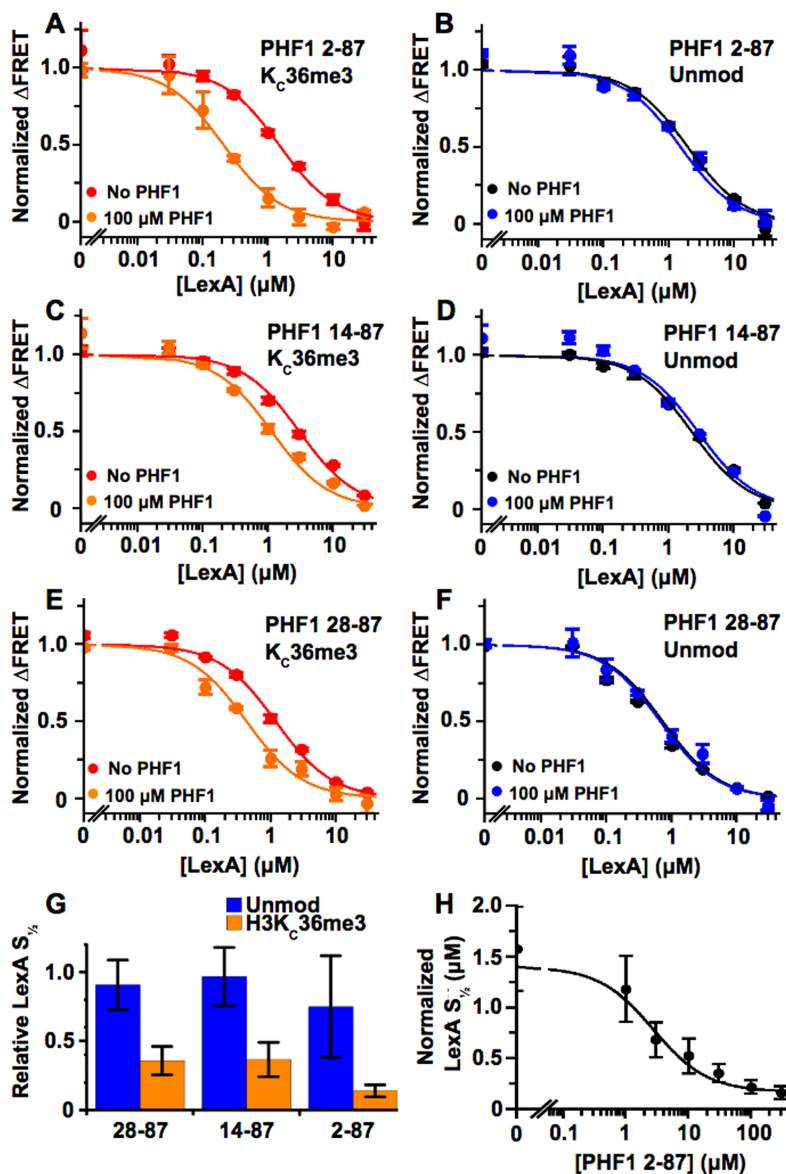
Figure 3. PHF1 NTD-Tudor increases accessibility of nucleosomal DNA by nearly an order of magnitude. (A, B) FRET efficiencies of LexA titrations with (orange and blue) or without (red or black) PHF1(2–87) held at a constant 100 μM with H3K$_C$36me3 (A) or unmodified (B) nucleosomes. (C–F) Like (A) and (B) but with PHF1(14–87) (**C** and **D**) or PHF1(28–87) (**E** and **F**). (**G**) LexA $S_{1/2}$ binding to H3K$_C$36me3 (orange) or unmodified (blue) with 100 μM PHF1 relative to no PHF1. (**H**) LexA $S_{1/2}$ shifts as a function of PHF1(2–87) concentration with H3K$_C$36me3 nucleosomes. LexA $S_{1/2}$ is normalized relative to the $S_{1/2}$ in the absence of PHF1(2–87).

sine 36 of H3 (H3K$_C$36me3). This modification has been shown to accurately mimic trimethyl-lysines (35). We then titrated PHF1(2–87), PHF1(14–87) and PHF1(28–87) with Cy3–Cy5 labeled nucleosomes. We find that each of these proteins do not have a significant effect on the FRET efficiency (Supplementary Figure S5). This result indicates that the binding by these PHF1 constructs do not shift the nucleosome into a predominately unwrapped state.

The PHF1 NTD enhances the impact of the Tudor domain on nucleosome accessibility

We previously determined that the binding of PHF1-Tudor domain to H3K$_C$36me3-containing nucleosomes increases

DNA accessibility within the nucleosome for a transcription factor, even though the histone interaction itself does not shift the nucleosome into a predominately unwrapped state (11). We therefore investigated whether the PHF1-NTD influences this PHF1 function. We generated the Cy3–Cy5 labeled nucleosomes where the LexA target site is inserted into the Widom 601 sequence from the 8th–27th base pairs, which positions the site near the Cy3 label. LexA can bind to its site when the nucleosome is partially unwrapped (30). So, as LexA is titrated with Cy3-Cy5 labeled nucleosomes, the FRET efficiency reduces as LexA binds to its site and traps the nucleosome in a partially unwrapped state (Figure 2C and Supplementary Figure S6). The nor-

malized change in FRET efficiency (ΔFRET) as a function of LexA concentration fits to non-cooperative binding isotherm, $E = 1/(1 + S_{1/2}/[LexA])$. $[LexA]$ is the concentration of LexA and $S_{1/2}$ is the concentration of LexA that changes the FRET efficiency by 50% of the total change. A reduction in the $S_{1/2}$ indicates that the accessibility within the nucleosome has increased.

To investigate the effect of PHF1-NTD, we prepared Cy3–Cy5 labeled nucleosomes that contained H3K$_C$36me3 and measured FRET in the presence of LexA at a concentration equal to the measured $S_{1/2}$ and either PHF1(2–87), PHF1(14–87) or PHF1(28–87). As expected, in the absence of PHF1, the normalized ΔFRET due to LexA binding to H3K$_C$36me3-nucleosomes is 0.5 (Figure 2C). We then titrated each of the PHF1 constructs and measured the normalized ΔFRET (Figure 2D). If the PHF1 truncation does not influence LexA binding, then the normalized ΔFRET should remain at 0.5. We find that the normalized ΔFRET decreases as the concentration of PHF1(28–87) increases, which indicates that the Tudor domain increases nucleosome accessibility, in agreement with our previous report (11). However, addition of PHF1(2–87) and PHF1(14–87) constructs caused a substantial increase in DNA accessibility. In fact, the normalized ΔFRET saturates in the PHF1(2–87) titration and results in an $S_{1/2} = 16 \pm 5\,\mu$M (see Materials and Methods for the fitting). These results reveal that that the PHF1-NTD dramatically enhances the ability of PHF1-Tudor to increase the DNA accessibility within the nucleosome.

The increased influence of PHF1-Tudor with the NTD on nucleosome accessibility is specific to H3K$_C$36me3 nucleosomes

The influence of the PHF1-Tudor domain on nucleosome accessibility depends on H3K$_C$36me3 (11). Since the NTD markedly enhances the increase of nucleosome accessibility induced by PHF1-Tudor, we investigated whether the combination of the PHF1 Tudor and N-terminal domains retained H3K$_C$36me3 specificity. We carried out separate PHF1(2–87), PHF1(14–87) and PHF1(28–87) titrations using unmodified Cy3–Cy5 labeled nucleosomes and a constant LexA concentration that is equal to the $S_{1/2}$ (Figure 2E). These titrations revealed a negligible shift in the normalized ΔFRET, whereas H3K$_C$36me3 nucleosomes showed a significant reduction of the normalized ΔFRET, as discussed above (Figure 2D). Together, these data indicate that the increase in nucleosome accessibility induced by the combination of PHF1 Tudor and NTD is specific to H3K$_C$36me3 nucleosomes.

The PHF1 NTD-Tudor increases the DNA-binding protein occupancy within the nucleosomes by nearly an order of magnitude

After determining that the linked NTD and Tudor significantly increased the DNA accessibility in H3K$_C$36me3-containing nucleosomes, we quantified these changes. To do this, we carried out the LexA titrations with Cy3–Cy5 labeled nucleosomes that contain H3K$_C$36me3 and a constant PHF1(2–87) concentration of 100 μM (Figure 3A). We chose this concentration because the impact of PHF1(2–87) on nucleosome accessibility is nearly saturated (Figure

2D). This LexA titration determines the $S_{1/2}$ of the LexA binding within H3K$_C$36me3 nucleosomes in the presence of PHF1(2–87). By comparing the $S_{1/2}$ of LexA binding to nucleosomes with ($S_{1/2\ PHF1(2-87)}^{K36me3} = 0.2 \pm 0.05\,\mu$M) and without ($S_{1/2\ no\ PHF1(2-87)}^{K36me3} = 1.5 \pm 0.3\,\mu$M) PHF1(2–87), we determined the relative binding probability to be $\frac{S_{1/2\ no\ PHF1(2-87)}^{K36me3}}{S_{1/2\ PHF1(2-87)}^{K36me3}}$ $= 8 \pm 2$. This can be converted to a change in binding free energy by:

$$\Delta G_{PHF1(2-87)}^{K36me3} - \Delta G_{no\ PHF1(2-87)}^{K36me3} = \Delta\Delta G_{PHF1(2-87)}^{K36me3} = -k_B T\,ln\left(\frac{S_{1/2\ no\ PHF1(2-87)}^{K36me3}}{S_{1/2\ PHF1(2-87)}^{K36me3}}\right) = -1.2 \pm 0.1\,\text{kcal/mol}.$$

k_B is the Boltzmann constant and T is room temperature. We controlled for LexA binding being directly impacted by PHF1(2–87) by detecting LexA binding to naked DNA with electromobility shift analysis (EMSA, Supplementary Figure S7), and find that PHF1(2–87) does not impact LexA binding. Interestingly, PHF1(2–87) impact on nucleosome accessibility is larger than the changes induced by other histone PTMs in the nucleosome entry–exit region such as H3K56ac (37) and H3Y41ph , and DNA sequence changes in the first seven base pairs of the nucleosome (31). However, combinations of these factors such as both H3K56ac and H3Y41ph increase accessibility similarly to that of PHF1(2–87) .

Our results shown in Figure 2 indicate that H3K$_C$36me3 is required for PHF1 to induce an 8-fold increase in nucleosome accessibility. To investigate this PTM dependence further, we carried out LexA titrations with unmodified nucleosomes and either with ($S_{1/2\ PHF1(2-87)} = 1.5 \pm 0.7\,\mu$M) or without ($S_{1/2\ no\ PHF1(2-87)} = 2.0 \pm 0.3\,\mu$M) 100 μM PHF1(2–87) (Figure 3B). We observed no significant change in the LexA $S_{1/2}$ using unmodified nucleosomes, which confirms that the PHF1 induced effect requires H3K$_C$36me3.

The entire PHF1 NTD is necessary to enhance DNA accessibility within the nucleosome.

Our observation that PHF1(2–87) has a larger impact than PHF1(14–87) and PHF1(28–87) on nucleosome FRET efficiency with constant LexA (Figure 2D) suggested that the PHF1 NTD increases the impact of PHF1-Tudor on nucleosome accessibility. To examine this, we carried out LexA titrations with 100 μM PHF1(14–87) and 100 μM PHF1(28–87) separately. We find that PHF1(14–87) and PHF1(28–87) decreases the LexA $S_{1/2}$ by 2.7 ± 0.8 ($\Delta\Delta\ G_{PHF1(14-87)}^{H3K_C36me3} = 0.59 \pm 0.18$ kcal/mol), and $S_{1/2}$ by 2.8 ± 0.9 ($\Delta\Delta\ G_{PHF1(28-87)}^{H3K_C36me3} = 0.61 \pm 0.20$ kcal/mol), respectively (Figure 3C and E). This implies that both PHF1 constructs have a similar 3-fold impact on DNA accessibility within the nucleosome. This data also suggest that the entire NTD is required to produce the enhancement. Similar titrations with unmodified nucleosomes again show no increased accessibility (Figure 3D and F) indicating that H3K$_C$36me3 is required for all three PHF1 constructs tested.
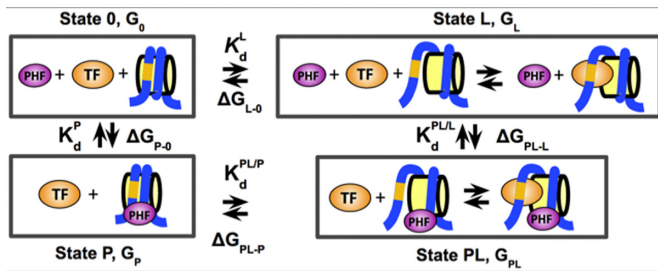
Figure 4. Model of PHF1 regulation of DNA accessibility within the nucleosome. A six-state model of TF binding to its target site within the nucleosome and PHF1 binding to H3K36me3. We simplify the model to a four-state model because our FRET system cannot differentiate between a partially unwrapped nucleosome bound or not bound by the TF.

A four-state binding model indicates that PHF1 preferentially interacts with unwrapped nucleosome by nearly an order of magnitude

To understand how PHF1 impacts nucleosome accessibility, we carried out separate LexA titrations with a range of PHF1(2–87) concentrations (Figure 3H). We then modeled the combined interactions of PHF1(2–87) and LexA with nucleosomes using a four-state model (Figure 4). We chose to use a four-state model where we combine the unwrapped LexA-free nucleosome state with the unwrapped LexA-bound nucleosome state for three reasons. (i) We cannot differentiate between an unwrapped nucleosome with and without either LexA or PHF1(2–87) bound. (ii) The site exposure equilibrium constant is the ratio of the concentration of the partially unwrapped nucleosome, which exposes the LexA binding site, divided by the wrapped nucleosome concentration, which protects the LexA binding site. This equilibrium constant is much less than 1 because the nucleosome unwraps with a low probability (29–30,32,40). So, the unwrapped LexA-free states are low probability states and should not contribute significantly to the population of states. (iii) This is the minimal model for three interacting molecules.

This model predicts that the LexA $S_{1/2}$ changes as $S_{1/2} = \frac{K_D^L K_D^{PL/P}(K_D^P + [P])}{K_D^P K_D^{PL/P} + K_D^L[P]}$, where K_D^L is the LexA dissociation constant without PHF1 and $K_D^{PL/P}$ is the LexA dissociation constant with PHF1 bound to the nucleosomes. We fit the change in LexA $S_{1/2}$ for increasing PHF1(2–87) concentrations to this functional form and find that $\frac{K_D^{PL/P}}{K_D^L}$ is 8 ± 2 (similar to the ratio previously found) and that K_D^P, the PHF1(2–87) dissociation constant without LexA, is 20 ± 10 μM, which is similar to our previous measurement with PHF1(28–87). An important aspect of this four-state model (Figure 4) is that the free energy difference between the nucleosome bound with LexA and PHF1(2–87) (State LP) and the unbound nucleosome state (State 0) must be the same whether LexA (State L) or PHF1(2–87) (State P) binds first. Therefore, $\Delta G_{PL-L} + \Delta G_{L-0} = \Delta G_{PL-P} + \Delta G_{P-0}$ and since $\Delta G = k_B T \ln(K_D)$: $\frac{K_D^{PL/P}}{K_D^L} = \frac{K_D^{PL/L}}{K_D^P}$. This implies that the relative binding affinity of LexA to nucleosomes with and without PHF1(2–87) is equal to the relative binding affinities of

PHF1(2–87) with and without LexA. We separately determined that PHF1(2–87) does not influence LexA binding to its target site within DNA (Supplementary Figure S7), which controls for a direct interaction between PHF1(2–87) and LexA. Therefore, we conclude that PHF1(2–87) binds partially unwrapped nucleosomes 8-fold higher than fully wrapped nucleosomes, which in turn significantly enhances DNA accessibility within the entry-exit region of the nucleosome.

The PHF1 Tudor domain regulates occupancy of DNA-binding complexes within the nucleosome by decreasing the dissociation rate

PHF1 could regulate DNA accessibility by two nonexclusive mechanisms. (i) PHF1 could increase the probability that a DNA site is exposed for binding, which would increase the binding rate and occupancy. (ii) PHF1 could decrease protein dissociation from its site once it is bound. We recently reported that nucleosomes can increase the rate of transcription factor dissociation from a target sites within nucleosomes by three orders of magnitude (38). This results in a dramatic reduction in TF occupancy. To determine which of these mechanisms PHF1 uses to increase LexA occupancy within the nucleosome, we carried out smFRET measurements (25). We used the same nucleosome constructs that were used in the ensemble measurements except that we included a 75 bp extension on the opposites side to where the LexA binding site is located (Figure 2A). Here, we detect single LexA binding and dissociation events to and from nucleosomes that are tethered to a quartz surface (Figure 5A) by observing changes in smFRET (Figure 5B) (26). By quantifying the dwell times in the high and low FRET states and then fitting the cumulative sum of the dwell time (Supplementary Figures S8–S10), we can determine the binding and dissociation rates of LexA. In the absence of PHF1, we find that with unmodified and H3K_C36me3 nucleosomes the binding rate increases linearly as a function of LexA concentration and the dissociation rate is constant as we previously reported for unmodified nucleosomes (38). In addition, the magnitude of the binding and dissociation rates without PHF1 are nearly identical (Supplementary Figure S11). This implies that H3K_C36me3 alone does not increase accessibility within the nucleosome, which is consistent with our ensemble FRET measurements (Figure 2C, (11)).

We then carried out smFRET experiments with PHF1(2–87) to determine its impact on both LexA binding and dissociation rates. Unfortunately, we found that in the presence of PHF1(2–87) tethered nucleosomes were not stable (data not shown), which does not agree with ensemble data (Supplementary Figure S5). This issue with the surface tethering of the nucleosomes prevented us from using smFRET measurements to determine the impact of PHF1(2–87) on LexA binding dynamics. However, we did find that up to 30 μM PHF1(14–87) and PHF1(28–87) did not destabilize tethered nucleosomes. Therefore, we carried out smFRET measurements of LexA binding with 30 μM of PHF1(14–87) and PHF1(28–87), separately. With either PHF1(14–87) or PHF1(28–87), we find that the LexA binding rates are linear with increasing LexA and that the dissociation rates are
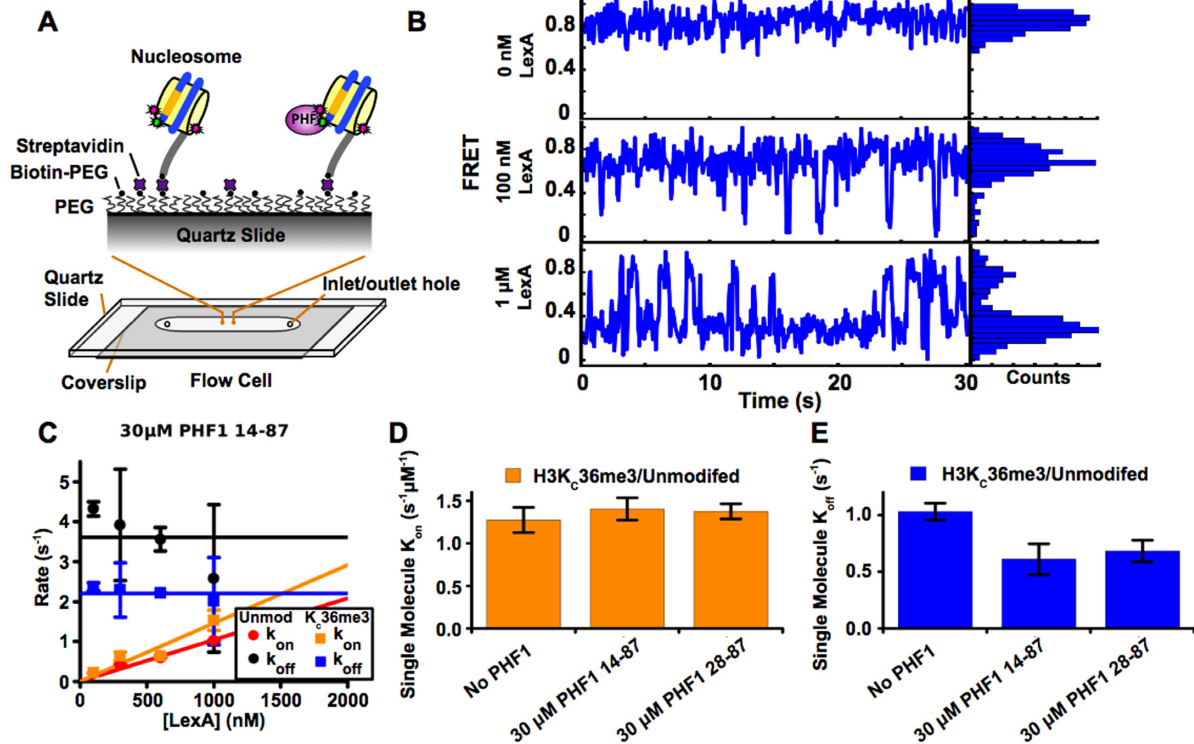
Figure 5. The Tudor domain increases accessibility by decreasing DNA-binding protein dissociation rates from nucleosomes. (**A**) Schematic of a single molecule flow cell. (**B**) Representative single molecule FRET traces with 0 (top), 100 nM (middle), and 1 μM (bottom) LexA. The evolution of a low FRET state is due to LexA trapping the nucleosome in an unwrapped state. (**C**) Rate constants of LexA binding to H3K$_C$36me3 (on: orange, off: blue) and unmodified (on: red, off: black). (D, E) Comparison of on (**D**) and off (**E**) rates of LexA with no PHF1, with 30 μM PHF1(14–87), and with 30 μM PHF1(28–87). Rates are shown H3K$_C$36me3 nucleosomes relative to unmodified nucleosomes. Off rates are fit to a flat line. On rates are fit to lines with 0 y-intercept. Error bars represent error in fits to cumulative sum distributions (see Supplementary Figures S8–S10).

constant (Figure 5C). We then compared the binding and dissociation rates of LexA with PHF1(14–87) or PHF1(28–87) to no PHF1. We find that the LexA binding rates are not impacted by 30 μM of either PHF1(14–87) or PHF1(28–87) (Figure 5D), while the LexA dissociation rates were reduced by a factor of 2.0 ± 0.2 and 1.7 ± 0.2 with PHF1(14–87) and PHF1(28–87), respectively (Figure 5E). The fact that we are limited to 30 μM of PHF1(14–87) and PHF1(28–87) in our smFRET measurements constrains what we can conclude about their influence on LexA binding. 30 μM of PHF1(14–87) and PHF1(28–87) is significantly below the concentration to fully saturate their impact on LexA occupancy (Figure 2D). Therefore, even though we do not observe a significant impact on the LexA binding rate, it is possible that higher concentrations of PHF1(14–87) and PHF1(28–87) would influence the LexA binding rate.

It is interesting that at subsaturating concentrations of PHF1(14–87) and PHF1(28–87) we observe a decrease in the LexA dissociation rate. The nucleosome occupancy of PHF1(14–87) and PHF1(28–87) will likely increase while LexA is transiently bound to the nucleosome. So, while the average nucleosome occupancy of PHF1(14–87) and PHF1(28–87) is subsaturating, it is expected to be higher while LexA is bound. Therefore, 30 μM of PHF1(14–87) and PHF1(28–87) could still impact the LexA dissociation rate, which is observed. These results indicate that the PHF1 Tudor domain increases LexA occupancy at least in

part by decreasing the dissociation rate. This highlights how controlling nucleosome induced protein dissociation can be used to regulate DNA accessibility within the nucleosome.

DISCUSSION

In this study, we quantitatively investigated the combined influence of the PHF1 N-terminal and Tudor domains on nucleosome accessibility, and find that together, they increase accessibility by nearly an order of magnitude. We then made two key observations about how PHF1 increases accessibility. First, we find that PHF1(2–87) increases nucleosome accessibility due to preferential binding to partially unwrapped nucleosomes that contain H3K$_C$36me3. This appears to be the first report of a histone PTM-recognizing protein that shows selectivity for a structurally altered nucleosome state. The location of H3K36 is important for the observed effect because (i) this residue protrudes between two sections of the nucleosomal DNA molecule near the entry-exit region (Figure 2B) and (ii) the PHF1 Tudor domain interacts with amino acids 32–39 of the H3 tail. While modeling indicates that the PHF1 Tudor domain can bind to fully wrapped nucleosomes containing H3K36me3 (11), our results indicate that PHF1 preferentially binds partially unwrapped nucleosomes. Also, the orientation of PHF1 Tudor bound to a fully wrapped nucleosome positions the PHF1 NTD away from the nucleosome so it cannot interact

directly with the nucleosome (Supplementary Figure S4B). This combined with our observation that the PHF1 NTD is important for increasing nucleosome accessibility suggests that the NTD likely interacts with the nucleosome only when it is unwrapped. The NTD could interact with the partially unwrapped nucleosome via contacts with the major groove of the DNA near the entry–exit region. These observations suggest that the PHF1-NTD may enhance LexA binding through DNA interactions. However, further studies are needed to fully reveal the mechanism by which the PHF1 NTD enhances nucleosome accessibility.

Our finding that PHF1 preferentially interacts with partially unwrapped nucleosomes suggests that PHF1 binding could function synergistically with other chromatin factors that impact DNA accessibility. We and others have reported that histone PTMs in the DNA entry-exit region (37,41–44) and DNA sequence (31,45–47) can individually and in combination (31) increase nucleosome accessibility. Perhaps, these PTMs and DNA sequence can function to regulate PHF1 binding to nucleosomes and/or function with PHF1 to regulate DNA accessibility. In addition, since some ATP dependent chromatin remodeling complexes partially unwrap nucleosomes (48), our results suggest that these remodeling complexes could also facilitate PHF1 binding to H3K36me3 containing nucleosomes. Finally, there are numerous histone PTM binding domains that recognize H3K36me3 (49). Our findings suggest that other H3K36me3 binding proteins may also impact nucleosome accessibility and that other factors that regulate DNA unwrapping within the entry-exit region of the nucleosome could regulate H3K36me3 recognition within the nucleosome.

Our second key observation here is that PHF1 Tudor enhances nucleosome accessibility by decreasing the dissociation rate of a DNA-binding protein. We recently reported that nucleosomes regulate DNA–protein interactions by increasing the rate of transcription factor dissociation from DNA by at least three orders of magnitude (38,49). A potential mechanism for this rate increase is that DNA–histone interactions compete with partially bound transcription factors (50). Our findings suggest that PHF1 Tudor may interfere with the competition between DNA-histone binding and DNA–TF binding thereby reducing the LexA dissociation rate. This work appears to be the first reported chromatin regulator controlling nucleosome accelerated protein dissociation, demonstrating the potential for regulating this nucleosome function. It will be interesting to determine if other H3K36me3 binding proteins also regulate nucleosome accessibility by impacting DNA–protein dissociation.

Finally, PHF1 is linked to transcription regulation and DNA repair, which both require enhanced DNA accessibility within chromatin. PHF1 can protect chromatin from transcriptional repression by PRC2 through its interaction with H3K36me3 (15,22–23,51–52), and it can facilitate transcription by promoting nucleosome unwrapping. PHF1 is also localized to chromatin sites containing a DNA double strand break together with the DNA repair regulators PARP1 and Ku70–Ku80 (15). Future studies are needed to determine how the two separate PHF1 properties: (i) interacting with regulatory complexes such as PRC2 and PARP1 and (ii) enhancing DNA accessibility, function together and if these two properties are functionally linked.

SUPPLEMENTARY DATA

Supplementary Data are available at NAR Online.

REFERENCES

1. Li,B., Bing,L., Michael,C. and Workman,J.L. (2007) The role of chromatin during transcription. *Cell*, **128**, 707–719.
2. Almouzni,G., Geneviève,A. and Howard,C. (2016) Maintenance of epigenetic information. *Cold Spring Harb. Perspect. Biol.*, **8**, a019372.
3. Sinha,M., Manisha,S. and Peterson,C.L. (2009) Chromatin dynamics during repair of chromosomal DNA double-strand breaks. *Epigenomics*, **1**, 371–385.
4. Zhao,Y. and Garcia,B.A. (2015) Comprehensive catalog of currently documented histone modifications. *Cold Spring Harb. Perspect. Biol.*, **7**, a025064.
5. Huang,H., Lin,S., Garcia,B.A. and Zhao,Y. (2015) Quantitative proteomic analysis of histone modifications. *Chem. Rev.*, **115**, 2376–2418.
6. Shema,E., Jones,D., Shoresh,N., Donohue,L., Ram,O. and Bernstein,B.E. (2016) Single-molecule decoding of combinatorially modified nucleosomes. *Science*, **352**, 717–721.
7. Strahl,B.D. and Allis,C.D. (2000) The language of covalent histone modifications. *Nature*, **403**, 41–45.
8. Jenuwein,T. and Allis,C.D. (2001) Translating the histone code. *Science*, **293**, 1074–1080.
9. Cosgrove,M.S., Boeke,J.D. and Wolberger,C. (2004) Regulated nucleosome mobility and the histone code. *Nat. Struct. Mol. Biol.*, **11**, 1037–1043.
10. Bowman,G.D. and Poirier,M.G. (2015) Post-translational modifications of histones that influence nucleosome dynamics. *Chem. Rev.*, **115**, 2274–2295.
11. Musselman,C.A., Gibson,M.D., Hartwick,E.W., North,J.A., Gatchalian,J., Poirier,M.G. and Kutateladze,T.G. (2013) Binding of PHF1 Tudor to H3K36me3 enhances nucleosome accessibility. *Nat. Commun.*, **4**, 2969.
12. Sarma,K., Margueron,R., Ivanov,A., Pirrotta,V. and Reinberg,D. (2008) Ezh2 requires PHF1 to efficiently catalyze H3 lysine 27 trimethylation in vivo. *Mol. Cell. Biol.*, **28**, 2718–2731.
13. Cao,R., Wang,H., He,J., Erdjument-Bromage,H., Tempst,P. and Zhang,Y. (2008) Role of hPHF1 in H3K27 methylation and hox gene silencing. *Mol. Cell. Biol.*, **28**, 1862–1872.
14. Hong,Z., Jiang,J., Lan,L., Nakajima,S., Kanno,S.-I., Koseki,H. and Yasui,A. (2008) A polycomb group protein, PHF1, is involved in the response to DNA double-strand breaks in human cell. *Nucleic Acids Res.*, **36**, 2939–2947.
15. Musselman,C.A., Nikita,A., Reiko,W., Abraham,C.G., Marie-Eve,L., Zehui,H., Christopher,A., Siddhartha,R., Nuñez,J.K., Jac,N. *et al.* (2012) Molecular basis for H3K36me3 recognition by the Tudor domain of PHF1. *Nat. Struct. Mol. Biol.*, **19**, 1266–1272.
16. Ballaré,C., Lange,M., Lapinaite,A., Martin,G.M., Morey,L., Pascual,G., Liefke,R., Simon,B., Shi,Y., Gozani,O. *et al.* (2012) Phf19 links methylated Lys36 of histone H3 to regulation of Polycomb activity. *Nat. Struct. Mol. Biol.*, **19**, 1257–1265.

17. Cai,L., Rothbart,S.B., Lu,R., Xu,B., Chen,W.-Y., Tripathy,A., Rockowitz,S., Zheng,D., Patel,D.J., Allis,C.D. *et al.* (2013) An H3K36 methylation-engaging Tudor motif of polycomb-like proteins mediates PRC2 complex targeting. *Mol. Cell*, **49**, 571–582.

18. Qin,S., Guo,Y., Xu,C., Bian,C., Fu,M., Gong,S. and Min,J. (2013) Tudor domains of the PRC2 components PHF1 and PHF19 selectively bind to histone H3K36me3. *Biochem. Biophys. Res. Commun.*, **430**, 547–553.

19. O'Connell,S., Wang,L., Robert,S., Jones,C.A., Saint,R. and Jones,R.S. (2001) Polycomblike PHD fingers mediate conserved interaction with enhancer of zeste protein. *J. Biol. Chem.*, **276**, 43065–43073.

20. Laible,G., Wolf,A., Dorn,R., Reuter,G., Nislow,C., Lebersorger,A., Popkin,D., Pillus,L. and Jenuwein,T. (1997) Mammalian homologues of the Polycomb-group gene Enhancer of zeste mediate gene silencing in Drosophila heterochromatin and at S. cerevisiae telomeres. *EMBO J.*, **16**, 3219–3232.

21. Beck,D.B., Bonasio,R., Kaneko,S., Li,G., Li,G., Margueron,R., Oda,H., Sarma,K., Sims,R.J., Son,J. *et al.* (2010) Chromatin in the nuclear landscape. *Cold Spring Harb. Symp. Quant. Biol.*, **75**, 11–22.

22. Gaydos,L.J., Rechtsteiner,A., Egelhofer,T.A., Carroll,C.R. and Strome,S. (2012) Antagonism between MES-4 and Polycomb repressive complex 2 promotes appropriate gene expression in C. elegans germ cells. *Cell Rep.*, **2**, 1169–1177.

23. Schmitges,F.W., Prusty,A.B., Faty,M., Stützer,A., Lingaraju,G.M., Aiwazian,J., Sack,R., Hess,D., Li,L., Zhou,S. *et al.* (2011) Histone methylation by PRC2 is inhibited by active chromatin marks. *Mol. Cell*, **42**, 330–341.

24. Clegg,R.M. (1992) Fluorescence resonance energy transfer and nucleic acids. *Methods Enzymol.*, **211**, 353–388.

25. Roy,R., Hohng,S. and Ha,T. (2008) A practical guide to single-molecule FRET. *Nat. Methods*, **5**, 507–516.

26. Luo,Y., North,J.A. and Poirier,M.G. (2014) Single molecule fluorescence methodologies for investigating transcription factor binding kinetics to nucleosomes and DNA. *Methods*, **70**, 108–118.

27. Bronson,J.E., Fei,J., Hofman,J.M., Gonzalez,R.L. and Wiggins,C.H. (2009) Learning rates and states from biophysical time series: a Bayesian approach to model selection and single-molecule FRET data. *Biophys. J.*, **97**, 3196–3205.

28. Lowary,P.T. and Widom,J. (1998) New DNA sequence rules for high affinity binding to histone octamer and sequence-directed nucleosome positioning. *J. Mol. Biol.*, **276**, 19–42.

29. Li,G., Gu,L., Marcia,L., Carlos,B. and Jonathan,W. (2004) Rapid spontaneous accessibility of nucleosomal DNA. *Nat. Struct. Mol. Biol.*, **12**, 46–53.

30. Li,G. and Widom,J. (2004) Nucleosomes facilitate their own invasion. *Nat. Struct. Mol. Biol.*, **11**, 763–769.

31. North,J.A., Shimko,J.C., Javaid,S., Mooney,A.M., Shoffner,M.A., Rose,S.D., Bundschuh,R., Fishel,R., Ottesen,J.J. and Poirier,M.G. (2012) Regulation of the nucleosome unwrapping rate controls DNA accessibility. *Nucleic Acids Res.*, **40**, 10215–10227.

32. Buning,R. and van Noort,J. (2010) Single-pair FRET experiments on nucleosome conformational dynamics. *Biochimie*, **92**, 1729–1740.

33. Sreerama,N. and Woody,R.W. (2000) Estimation of protein secondary structure from circular dichroism spectra: comparison of CONTIN, SELCON, and CDSSTR methods with an expanded reference set. *Anal. Biochem.*, **287**, 252–260.

34. Luger,K., Rechsteiner,T.J. and Richmond,T.J. (1999) Preparation of nucleosome core particle from recombinant histones. *Methods Enzymol.*, **304**, 3–19.

35. Simon,M.D., Chu,F., Racki,L.R., de la Cruz,C.C., Burlingame,A.L., Panning,B., Narlikar,G.J. and Shokat,K.M. (2007) The site-specific installation of methyl-lysine analogs into recombinant histones. *Cell*, **128**, 1003–1012.

36. Brehove,M., Wang,T., North,J., Luo,Y., Dreher,S.J., Shimko,J.C., Ottesen,J.J., Luger,K. and Poirier,M.G. (2015) Histone core phosphorylation regulates DNA accessibility. *J. Biol. Chem.*, **290**, 22612–22621.

37. Shimko,J.C., North,J.A., Bruns,A.N., Poirier,M.G. and Ottesen,J.J. (2011) Preparation of fully synthetic histone H3 reveals that acetyl-lysine 56 facilitates protein binding within nucleosomes. *J. Mol. Biol.*, **408**, 187–204.

38. Luo,Y., North,J.A., Rose,S.D. and Poirier,M.G. (2014) Nucleosomes accelerate transcription factor dissociation. *Nucleic Acids Res.*, **42**, 3017–3027.

39. Little,J.W., Baek,K., Roland,K.L., Smith,M.H., Lih-Ling,L. and Slilaty,S.N. (1994) [20]Cleavage of LexA repressor. In: *Methods in Enzymology*. pp. 266–284.

40. Koopmans,W.J.A., Buning,R., Schmidt,T. and van Noort,J. (2009) spFRET using alternating excitation and FCS reveals progressive DNA unwrapping in nucleosomes. *Biophys. J.*, **97**, 195–204.

41. Neumann,H., Hancock,S.M., Buning,R., Routh,A., Chapman,L., Somers,J., Owen-Hughes,T., van Noort,J., Rhodes,D. and Chin,J.W. (2009) A method for genetically installing site-specific acetylation in recombinant histones defines the effects of H3 K56 acetylation. *Mol. Cell*, **36**, 153–163.

42. Simon,M., North,J.A., Shimko,J.C., Forties,R.A., Ferdinand,M.B., Manohar,M., Zhang,M., Fishel,R., Ottesen,J.J. and Poirier,M.G. (2011) Histone fold modifications control nucleosome unwrapping and disassembly. *Proc. Natl. Acad. Sci. U.S.A.*, **108**, 12711–12716.

43. Casadio,F., Lu,X., Pollock,S.B., LeRoy,G., Garcia,B.A., Muir,T.W., Roeder,R.G. and Allis,C.D. (2013) H3R42me2a is a histone modification with positive transcriptional effects. *Proc. Natl. Acad. Sci. U.S.A.*, **110**, 14894–14899.

44. Di Cerbo,V., Mohn,F., Ryan,D.P., Montellier,E., Kacem,S., Tropberger,P., Kallis,E., Holzner,M., Hoerner,L., Feldmann,A. *et al.* (2014) Acetylation of histone H3 at lysine 64 regulates nucleosome dynamics and facilitates transcription. *Elife*, **3**, e01632.

45. Anderson,J.D. and Widom,J. (2000) Sequence and position-dependence of the equilibrium accessibility of nucleosomal DNA target sites. *J. Mol. Biol.*, **296**, 979–987.

46. Ngo,T.T.M., Zhang,Q., Zhou,R., Yodh,J.G. and Ha,T. (2015) Asymmetric unwrapping of nucleosomes under tension directed by DNA local flexibility. *Cell*, **160**, 1135–1144.

47. Hall,M.A., Shundrovsky,A., Bai,L., Fulbright,R.M., Lis,J.T. and Wang,M.D. (2009) High-resolution dynamic mapping of histone-DNA interactions in a nucleosome. *Nat. Struct. Mol. Biol.*, **16**, 124–129.

48. Narlikar,G.J., Sundaramoorthy,R. and Owen-Hughes,T. (2013) Mechanisms and functions of ATP-dependent chromatin-remodeling enzymes. *Cell*, **154**, 490–503.

49. Musselman,C.A., Khorasanizadeh,S. and Kutateladze,T.G. (2014) Towards understanding methyllysine readout. *Biochim. Biophys. Acta*, **1839**, 686–693.

50. Chen,C. and Bundschuh,R. (2014) Quantitative models for accelerated protein dissociation from nucleosomal DNA. *Nucleic Acids Res.*, **42**, 9753–9760.

51. Li,X., Isono,K.-I., Yamada,D., Endo,T.A., Endoh,M., Shinga,J., Mizutani-Koseki,Y., Otte,A.P., Casanova,M., Kitamura,H. *et al.* (2011) Mammalian polycomb-like Pcl2/Mtf2 is a novel regulatory component of PRC2 that can differentially modulate polycomb activity both at the Hox gene cluster and at Cdkn2a genes. *Mol. Cell. Biol.*, **31**, 351–364.

52. Yuan,W., Xu,M., Huang,C., Liu,N., Chen,S. and Zhu,B. (2011) H3K36 methylation antagonizes PRC2-mediated H3K27 methylation. *J. Biol. Chem.*, **286**, 7983–7989.